ELSEVIER

Nuclear Instruments and Methods in Physics Research A 442 (2000) 187–192

NUCLEAR INSTRUMENTS & METHODS IN PHYSICS RESEARCH Section A

www.elsevier.nl/locate/nima

Limited Geiger-mode microcell silicon photodiode: new results

G. Bondarenko[a], P. Buzhan[a], B. Dolgoshein[a,*], V. Golovin[b], E. Guschin[a], A. Ilyin[a], V. Kaplin[a], A. Karakash[a], R. Klanner[c], V. Pokachalov[a], E. Popova[a], K. Smirnov[a]

[a] *Moscow Engineering and Physics Institute (MEPHI), Moscow, Russian Federation*
[b] *Centre of Perspective Technology and Apparatus (CPTA), Moscow, Russian Federation*
[c] *Hamburg University/DESY, Germany*

Abstract

Recent results on Limited Geiger-mode Microcell Silicon Photodiode (LGP) are described. Two new modifications of LGP have been designed and produced. Each of them consists of 10^4 pixels 10×10 μm^2 size with area of 1 mm^2. These pixels operate as an independent photon counters, giving the output signal as a sum of the signals from pixels fired by photons. The effective "gain" is large ($\approx 10^5$). The efficiency of the visible light photon detection of few percents has been measured. Low-temperature dark rate dependence has been studied. The timing by LGP at the level of 100 ps (FWHM) was found.

1. Introduction

The single-photon silicon avalanche diode (SPAD) is a well-known device, which have been studied during many years [1–3]. The SPAD is a small (20–500 μm size) pixel photodiode which operates under bias voltage of 10–20% more than breakdown voltage, so each carrier generated by photons or thermally gives rise a Geiger-type discharge. This Geiger discharge is stopped due to drop of voltage below breakdown value either passively by external resister or actively by special quenching electronics. The total charge generated in Geiger discharge is determined by the charge accumulated in SPAD capacity (typically of few pF) and equal usually ~ 10 pC ($\sim 10^8$ electrons); that is the effective "gain" of the SPAD is about of 10^8.

It is very attractive to join many pixels together on the common silicon substrate, having their independent operation. The possible technological solution has been proposed firstly in Ref. [4] and checked experimentally in other papers [5,6].

Topologically such a photodiode has a metal–resistor–semiconductor structure (MRS-system) where the resistive layer (usually silicon carbide) serves as a decoupling element between of individual pixels. As an example Fig. 1 shows such a photodiode structure [7] which we call Limited Geiger-mode Microcell Silicon Photodiode (LGP) – the name based on its operational principle.

In comparison with Geiger SPAD each LGP pixel has much smaller capacity (typically of few fmF), so the total "gain" of each LGP pixel (total Geiger-mode charge) is of order 10^5. Actually each LGP pixel operates as independent photon Geiger counter; the pixel signal does not depend on primary ionization which fired this pixel. All LGP

* Corresponding author.
E-mail address: boris@mail.cern.ch (B. Dolgoshein)

0168-9002/00/$ - see front matter
PII: S0168-9002(99)01219-X

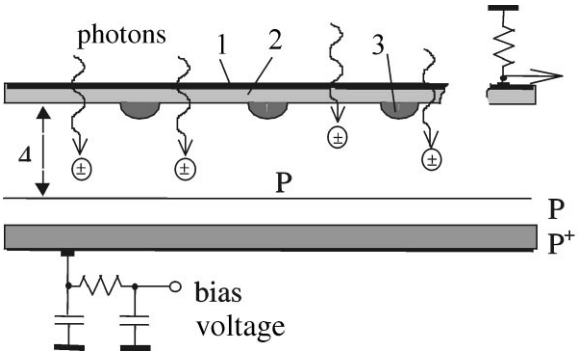

Fig. 1. The schematic photodiode structure: (1) semitransparent metal contact (Ti), $d \approx 100$ A; (2) SiC layer, $d \approx 0.15$ μm, $\rho = 10^5$–$10^7\,\Omega$ cm; (3) n^+, r or hemisphere ≈ 1.5 μm; (4) depletion region (epitaxial layer).

pixels work together on common load, so the output is a sum of the signals from all pixels fired [7]:

$$n_{\text{pixels fired}} = n_{\text{pixels total}}(1 - e^{-\epsilon N_{\text{photons}}/n_{\text{pixels total}}})$$

where ϵ is the photon detection efficiency. The LGP topology which is shown on Fig. 1 we will refer below as a modification "0".

2. The improvement of the LGP topology

The efficiency of photon detection for multypixel LGP structure is

$$\epsilon = QE\epsilon_G$$

where QE is quantum efficiency typically 0.5–0.8 and ϵ_G the probability for the carrier created by photon in depletion region to initiate a Geiger-mode discharge. The last one for high overvoltages ($\approx 10\%$) is determined by "geometrical" efficiency, that is a part of total LGP area occupied by n^+-pins (anodes), where the electric field is large enough for Geiger-mode performance. For LGP in Fig. 1 [7] such "geometrical" efficiency is only 3.6%, so the total photon detection efficiency ϵ is quite small ($\sim 1\%$). Unfortunately the simple way to increase ϵ just increasing the n^+-pins density does not help, because the higher n^+-pins density leads to strong coupling between neighbour pixels, deteriorates the pixels independency and limited Geiger-mode performance.

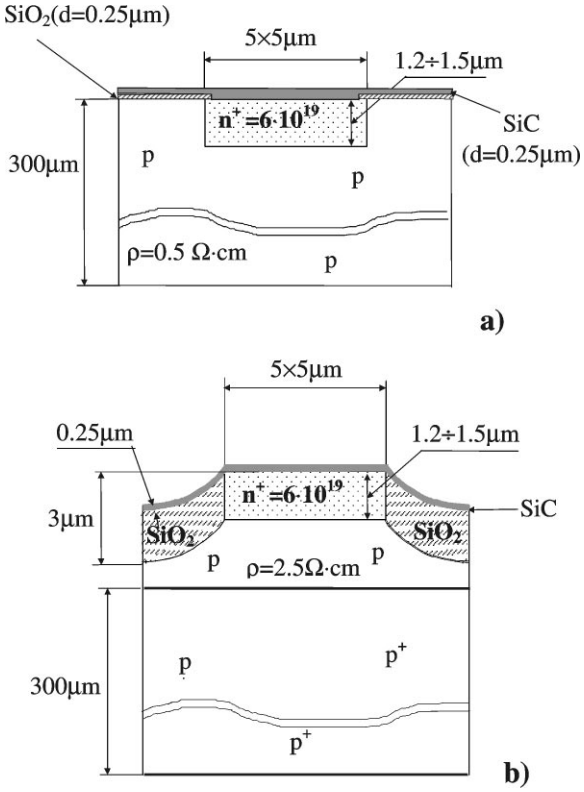

Fig. 2. Improved LGP topology: (a) Plane geometry (modification 1); (b) Mesotopology with p-epitaxy (modification 2).

In order to reduce the pixel–pixel coupling the improved LGP topology have been realized [8] (Fig. 2), referred below as modifications 1 and 2. They contain an additional SiO_2 layer for conventional planar (mod. 1) and mesostructure (mod. 2) and have the "geometrical" efficiency of about 25%.

The experimental set-up for LGP measurements is described in our previous paper [7]. In addition to that we use a special cryostat for low-temperature (down to nitrogen temperatures) measurements.

3. Limited Geiger-mode photodiode performance

3.1. Amplitude resolution

Fig. 3 shows two LGP spectra at different temperatures for low-intensity LED pulses. One can

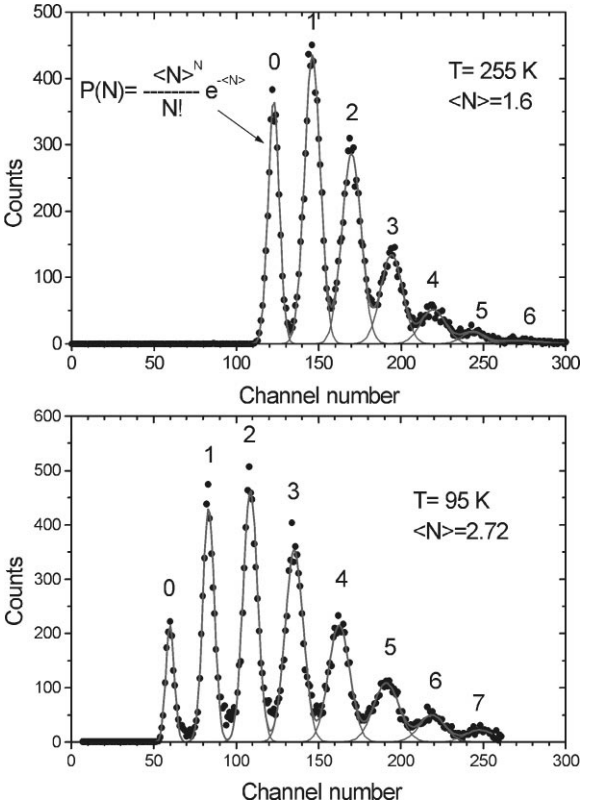

Fig. 3. Examples of the LGP amplitude spectra for low-intensity light pulses.

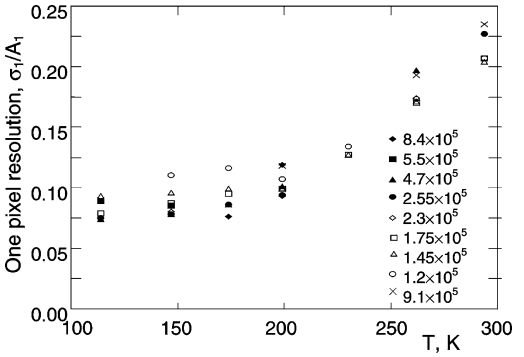

Fig. 4. Intrinsic single-pixel amplitude resolution σ_1/A_1 for LGP mod. "0" versus temperature.

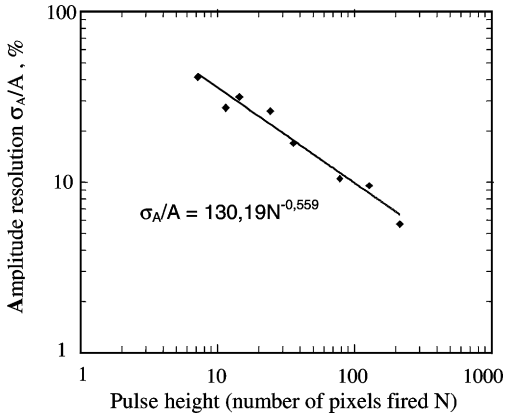

Fig. 5. LGP (mod. "0") amplitude resolution σ_A/A as a function of the number of pixels fired.

see that the relative intrinsic dispersion σ_1/A_1 of the single pixel signal is quite small, that is the different pixel signals are quite uniform ($\sigma_1/A_1 \simeq 0.15$). The decrease of the temperature (Fig. 4) reduces the σ_1/A_1 value down to 7–8%. The relative LGP amplitude resolution σ_A/A for more intensive light pulses is determined by the number of pixels fired:

$$\frac{\sigma_A}{A} = \frac{1}{\sqrt{n_{\text{pixels fired}}}}\sqrt{1+\left(\frac{\sigma_1}{A_1}\right)^2}.$$

Indeed Fig. 5 shows that σ_A/A is quite close to $1/\sqrt{n_{\text{pixels fired}}}$ dependence.

3.2. The dependence of the LGP signal on overvoltage

Each LGP pixel Geiger-type signal is limited due to local (within single pixel) drop of the bias voltage V below the V_0 where Geiger-mode discharge is stopped. That is the single pixel signal is determined by the total charge collected during the Geiger discharge of the single-pixel capacity C_0

$$\Delta Q = C_0(V - V_0)$$

where $\Delta V = (V - V_0)$ is overvoltage. Fig. 6 demonstrates $\Delta Q = C_0 \Delta V$ dependence which take a place up to overvoltages, where pixel–pixel decoupling is violated and C_0 becomes to increase with ΔV.

3.3. LGP photon detection efficiency

Photon detection efficiency $\epsilon = QE\epsilon_G$ has been measured for LGP configuration 1 and 2 using

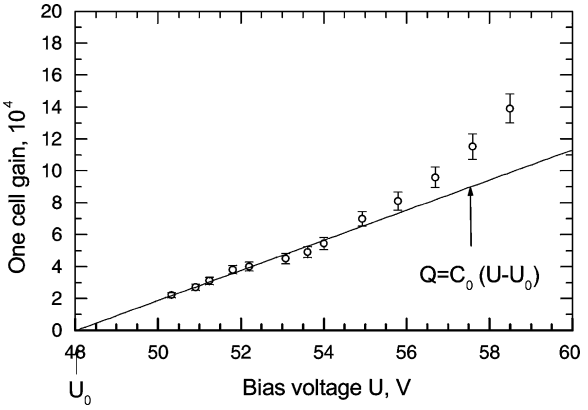

Fig. 6. LGP (mod. 2) "gain" (number of the carriers for single pixel fired) versus bias voltage.

different light sources and is shown in Fig. 7. The results agree satisfactorily with value $\epsilon_G \approx$ "geometrical" efficiency (25%) and expected quantum efficiency for visible light taking into account the light absorption in relatively thick n^+ layer (see Fig. 2). This absorption is especially sufficient for short wavelength part of the spectrum.

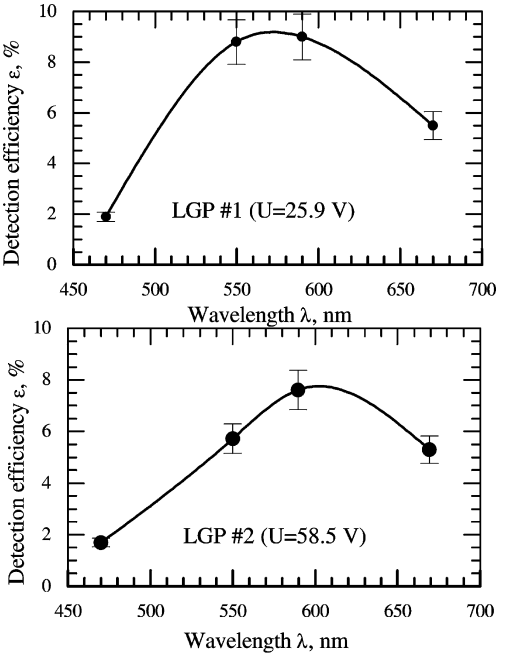

Fig. 7. Photon detection efficiency for different wavelength: (top) LGP mod. 1; (bottom) LGP mod. 2.

3.4. LGP dark rate

One of the important features of the LGP is high dark rate, originated from carriers, created in sensitive LGP volume by thermal emission, which can be strongly enhanced by high electric field [9].

Fig. 8 shows the strongly reduction of the LGP dark rate from ~ 10 MHz for room temperature to ~ 10 Hz for nitrogen temperature. However such a reduction of the LGP rate is much slower then its expected behaviour for pure thermal emission (see Fig. 8), apparently due to effects of high electric fields [9].

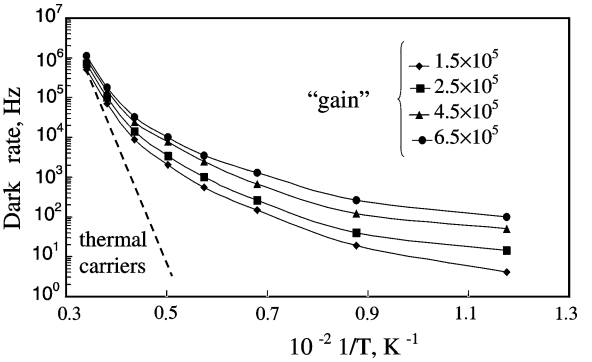

Fig. 8. LGP (mod. "0") dark rate versus temperature for different LGP "gains". Dashed line shows expected thermal carrier rate.

3.5. LGP recovery time

After the stoppage of the Geiger discharge in given pixel the local bias voltage is recovering to working bias voltage V. This recovery process can go in two stages:

- The charge collected in pixel capacity C_0 leaks to the neighbour pixels due to certain coupling between them. Time constant of this process depends on how strong this coupling is. As a result the voltage of many (all) LGP pixels becomes lower than working bias voltage V and efficiency and "gain" of the LGP during this process is lowering.

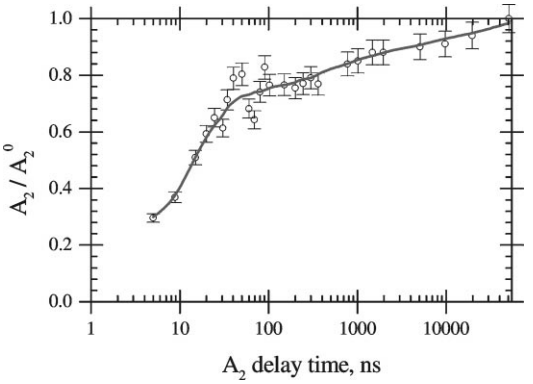

Fig. 9. LGP (mod. 2) recovery time studies: the amplitude of the second light pulse as a function of delay time from first one.

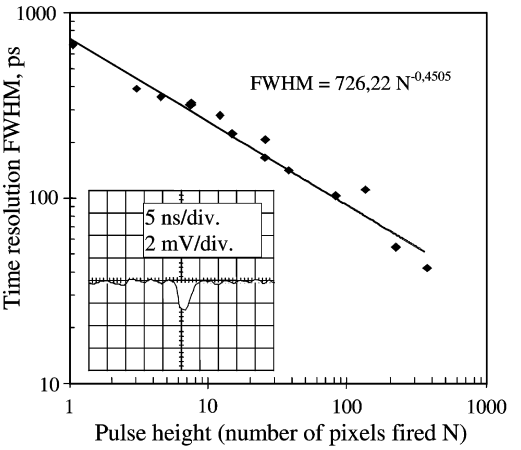

Fig. 10. Upper limit of the LGP (mod. "0") time resolution (FWHM) as a function of the number of the pixels fired.

- The second stage is the total recovery of bias voltage V with a time constant, determined by the resistance ("varistance") of the SiC layer.

The recovery time has been measured using two short pulse light sources delayed relative each other (Fig. 9). The intensity of the first pulse was large enough in order to fire $\sim 70\%$ of all LGP pixels. Fig. 9 shows two stages of the LGP recovery for large light intensity, when considerable part of LGP pixels are fired. For small light intensity ($n_{\text{fired}} \ll n_{\text{total}} = 10^4$) the first stage of the recovery is mostly sufficient and real recovery time has to be much smaller (≤ 10 ns).

3.6. Timing by LGP

Because the development of the Geiger-type discharge is estimated as very short ($\sim 10^{-10}$ s) Geiger-mode silicon photodiodes look very promising as a timing devices. For instance, the best timing obtained with Single Photon Avalanche Counters (SPAD) [10] is 20 ps FWHM. Therefore the timing by means of LGP's is expected also to be very good.

The 660 nm laser source with the pulse FWHM $\simeq 700$ ps has been used for LGP timing measurements. Fig. 10, displays the LGP time resolution versus number of pixels fired, that is versus laser light intensity. One can see from Fig. 10 the LGP time resolution follows the $1/\sqrt{n_{\text{pixel fired}}}$ dependence (as expected). On the other hand for the intrinsic LGP time resolution (for single pixel) this measurement can be considered as upper limit FWHM < 700 ps, because this value is determined by the laser pulse FWHM. The more short pulse laser is needed for more accurate measurements.

4. Conclusions

Different modifications of Limited Geiger-mode Photodiode have been studied. LGP is actually the system of many ($\sim 10^4$ mm^{-2}) photon microcounters. The LGP features are:

- signal from one pixel is $\simeq 10^5$ e, so electronics noise is negligible;
- good single pixel signal resolution $\sigma_A/A \sim 0.1$;
- low recovery time for low-intensity light pulses;
- LGP signal is very fast (~ 1 ns),

$$\text{timing} < \frac{700 \text{ ps}}{\sqrt{n_{\text{pixel fired}}}},$$

- relatively low photon detection efficiency (few %) has been found for modification studied;
- relatively high level of the dark rate $\sim 10^4$ mm^{-2} at -40°C temperature.

We hope that the last two points can be improved at the next technological steps we are planning.

References

[1] F. Zappa et al., Opt. Eng. 35 (4) (1996) 938 and references therein.
[2] S. Cowa et al., Appl. Phys. 35 (1996) 1956 and references therein.
[3] H. Dautet et al., Appl. Opt. 32 (1993) 3894 and references therein.
[4] V. Golovin et al., Patent of Russia N 1644708, 1989.
[5] N. Bacchetta et al., Nucl. Instr. and Meth. A 387 (1997) 225 and references therein.
[6] A. Akindinov et al., Nucl. Instr. and Meth. A 387 (1997) 231 and references therein.
[7] G. Bondarenko et al., Nuclear Phys. B (Proc. Suppl.) 61B (1998) 347.
[8] G. Bondarenko, V. Golovin, M. Tarasov, Claim at Patent of Russia N 98117319 from 22.09.98.
[9] G. Vincent et al., J. Appl. Phys. 50 (1979) 5984.
[10] S. Cowa et al., Rev. Sci. Instrum. 60 (1989) 1104.